

Stabilizing GANs with Octave Convolutions

Ricard Durall^{1,2} Franz-Josef Pfreundt¹ Janis Keuper^{1,3}
¹Fraunhofer ITWM, Germany
²IWR, University of Heidelberg, Germany
³Fraunhofer Center Machine Learning, Germany

Abstract

In this preliminary report, we present a simple but very effective technique to stabilize the training of CNN based GANs. Motivated by recently published methods using frequency decomposition of convolutions (e.g. Octave Convolutions), we propose a novel convolution scheme to stabilize the training and reduce the likelihood of a mode collapse. The basic idea of our approach is to split convolutional filters into additive high and low frequency parts, while shifting weight updates from low to high during the training. Intuitively, this method forces GANs to learn low frequency coarse image structures before descending into fine (high frequency) details. Our approach is orthogonal and complementary to existing stabilization methods and can simply be plugged into any CNN based GAN architecture. First experiments on the CelebA dataset show the effectiveness of the proposed method.

1. Introduction

Convolutional Neural Networks (CNNs) have achieved remarkable success in many computer vision domains such as classification [19, 18, 32], semantic segmentation [23, 31, 4], object detection [9, 30, 29] and image generation [17, 10, 27]. The basic architectural design of a CNN starts processing on a high resolution input, where filters examine small local pieces. Through stacking many different types of layers, especially convolutional ones, the receptive fields slowly grow with depth, and eventually encompass the entire input. Recent efforts have focus on improving the convolutional layers by reducing their inherent redundancy in both dense model parameters and in the channel dimension of feature maps [12, 24, 6, 33, 15, 5]. Standard convolutional layers are the key element on such an architecture. They are designed to detect local conjunctions of features from the previous layer and mapping their appearance to a feature map, which have always the same spatial resolution. However, natural images can be factorized into a low frequency signal that captures the global layout and

coarse structure, and a high frequency part that captures fine details. Attracted by the idea of having feature maps with different resolutions and breaking with standard convolutional layers, some works [15, 5] have built schemes, on top of standard CNNs architecture, that have access to different frequency content within the same feature map.

In recent years, unsupervised learning with CNNs has received a lot of attention in computer vision applications. In particular, learning reusable feature representations from large unlabeled datasets has been a very active area of research. In the context of computer vision, it is possible to leverage the huge amount of unlabeled data (images and videos) to learn good intermediate representations, which can then be used on a wide variety of supervised learning tasks. One successful way to build good image representations is by training Generative Adversarial Networks (GANs) [10]. GANs have achieved state-of-the-art results at generating realistic and crispy sharp looking images.

Unlike other generative techniques [17, 27] that model explicitly maximum likelihood, GANs provide an attractive alternative that allows to model implicitly the density. One can even argue that their learning process and the lack of a heuristic cost function are attractive to representation learning. Nonetheless, despite their success, GANs have a challenging unstable training and there is little to no theory explaining this behaviour. This makes it extremely hard to experiment with new variants, or to employ them in new domains, which drastically limits their applicability. In the literature, we encounter many current papers dedicated to finding heuristically stable architectures [28, 14, 2, 20], loss functions [25, 1, 11] or regularization strategies [26].

In this paper, we propose to replace standard convolution with octave convolution [5]. This replacement will have almost no impact on the architecture since octave convolution are orthogonal and complementary to existing methods that also focus on building better CNN topology. We apply our model to the CelebA [22] dataset, and we demonstrate that by simply substituting the convolutional layers, we can consistently improve the performances leading to a more stable

training, reducing the mode collapse. Overall, our contributions are summarized as follows:

- We propose OC-GAN, a novel and generalizable scheme for generative adversarial network that leads to more stable trainings.
- We achieve to reduce spatial redundancy by using octave convolution, and therefore, the training experiments a speedup.
- By employing a set of different scheme baselines, we assess the stability of our proposal providing both quantitative and qualitative results on CelebA dataset.

2. Related Work

Most of the deep learning approaches in computer vision are based on standard CNNs. They have heavily contributed in semantic image understanding tasks including the aforementioned works and references therein. In this work, we look at image generation techniques and we briefly review the seminal work in that direction. In particular, we focus our attention on a set of well-known GANs and the impact of alternative convolutional layers on these models.

2.1. Generative Adversarial Networks

The goal of generative models is to match real data distribution p_{data} with generated data distribution p_g . Thus, minimizing differences between two distributions is a crucial point for training generative models. Goodfellow *et al.* introduced an adversarial framework (GAN) [10] which is capable of learning deep generative models by minimizing the Jensen-Shannon Divergence between p_{data} and p_g . This optimization problem can be described as a minmax game between the generator G , which learns how to generate samples which resemble real data, and a discriminator D , which learns to discriminate between real and fake data. Throughout this process, G indirectly learns how to model p_{data} by taking samples z from a fixed distribution p_z (e.g. Gaussian) and forcing the generated samples $G(z)$ to match p_g . The objective loss function is defined as

$$\min_G \max_D \mathcal{L}(D, G) = \mathbb{E}_{\mathbf{x} \sim p_{\text{data}}} [\log(D(\mathbf{x}))] + \mathbb{E}_{z \sim p_z} [\log(1 - D(G(z)))]. \quad (1)$$

Deep Convolutional GAN. Deep Convolutional GAN (DCGAN) [28] is one of the popular and successful network topology design for GAN that in a certain way achieves a consistently stability during training. It is a direct extension of the GAN described above, except that it is mainly composed of convolutional and convolutional-transpose layers without max pooling or fully connected layers in both discriminator and generator.

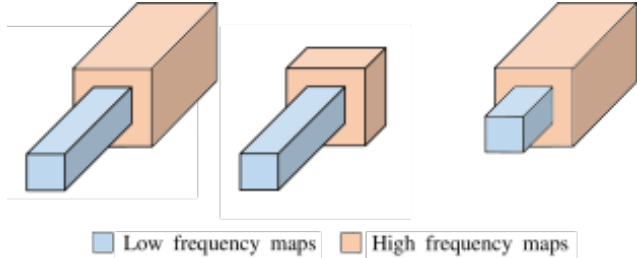


Figure 1: The hyper-parameters β s can be seen as a kind of virtual α since they can achieve similar performance by weighting the feature maps. (Left) β s are balanced. (Center) $\beta_L \geq \beta_H$. (Right) $\beta_H \geq \beta_L$.

Least-Squares GAN. Least-Squares GAN (LSGAN) [25] also tries to minimize Pearson X^2 divergence between the real and the generated distribution. The standard GAN uses a sigmoid cross entropy loss for the discriminator to determine whether its input comes from p_{data} and p_g . Nonetheless, this loss has an important drawback. Given a generated sample is classified as real by the discriminator, then there would be no apparent reason for the generator to be updated even though the generated sample is located far from the real data distribution. In other words, sigmoid cross entropy loss can barely push such generated samples towards real data distribution since its classification role has been achieved. Motivated by this phenomenon, LSGAN replaces a sigmoid cross entropy loss with a least square loss, which directly penalizes fake samples by moving them close to the real data distribution.

Wasserstein GAN. Wasserstein GAN (WGAN) [1] suggests the Earth-Mover (EM) distance which is also called the Wasserstein distance, as a measure of the discrepancy between the two distributions. The benefit of the EM distance over other metrics is that it is a more sensible objective function when learning distributions with the support of a low-dimensional manifold. EM distance is continuous and differentiable almost everywhere under Lipschitz condition, which standard feed-forward neural networks satisfy. In order to enforce such a condition, weight clipping is used on each neural network layer. Its main idea is to clamp the weight to a small range, so that the Lipschitz continuity is guaranteed. Finally, since EM distance is intractable, it is converted in to a tractable equation via Kantorovich-Rubinstein duality with the Lipschitz function.

2.2. Convolutional Layers

Standard convolutional layers are designed to detect local conjunctions of features from the previous layer and mapping their appearance to a feature map which does not vary its spatial resolution at no time. Nevertheless, in ac-

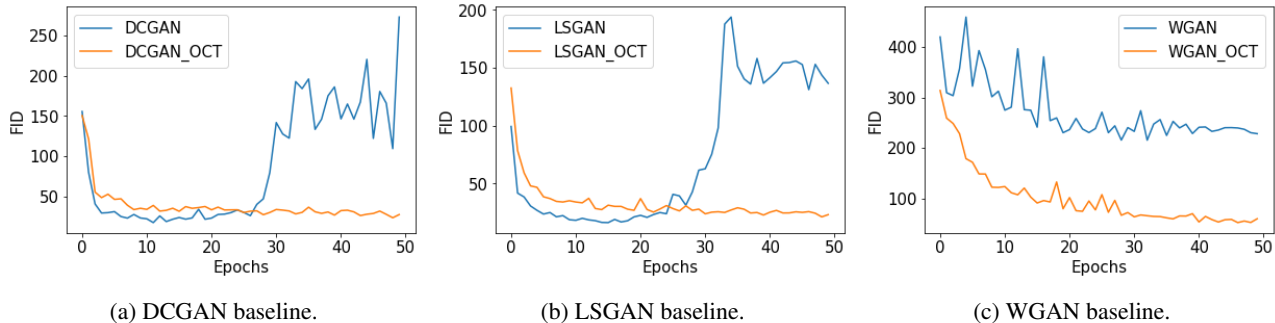


Figure 2: Each figure shows the FID evolution along the training using a certain GAN implementation and its octave variant.

cordance with the spatial-frequency model [3, 7], natural images can be factorized into a low frequency signal that captures the global layout and coarse structure, and a high frequency signal that captures fine details. Attracted by the idea of having feature maps with different resolution, recent works based on deep learning approaches [15, 5], have built on top of standard CNNs, architecture schemes that have access to different frequency content. A multigrid architecture is the idea suggested by [15] that has the intention of wiring cross-scale connections into network structure at the lowest level. In order to create such a topology, every convolutional filter extends spatially within grids (h, w) , across grids multiple scales (s) within a pyramid, and over corresponding feature channels (c) . Building in this fashion, a combination of pyramids across the architecture (h, w, s, c) .

In a similar manner, given the input feature tensor of a convolutional layer $X \in \mathbb{R}^{c \times h \times w}$, [5] suggest to factorize it along channel dimension into two groups, one for low frequencies and one for high frequencies $X = \{X^H, X^L\}$ arguing that the subset of the feature maps that capture spatially low frequency changes, contains spatially redundant information. In order to reduce the spatial redundancy, they introduce the octave feature representation, which corresponds to a division of the spatial dimensions by 2.

3. Method

In the following section, we describe OC-GAN approach which addresses the integration of octave convolution in GANs and the employed architecture for our proposed method.

3.1. Octave Convolution

The octave convolutional layers [5] split their feature maps into low frequency maps and high frequency maps $X = \{X^H, X^L\}$. In this fashion, those parts of the image that change rapidly from one color to another (e.g. sharp edges) and contain fine details, are captured by X^H . And those, who have parts that change gradually in the spatial dimensions (e.g. large surfaces with solid colors), are cap-

tured by the low frequency maps X^L . In practice, to produce the two frequency blocks, the spatial dimensions of the X^L feature representation are divided by a factor of 2. This helps each convolutional layer to capture more contextual information from distant locations and can potentially improve recognition performances.

The price for having such a octave convolutional architecture is an additional hyper-parameter $\alpha \in [0, 1]$ which denotes the ratio of low frequency part. Accordingly, the feature maps can be written as

$$X^L \in \mathbb{R}^{\alpha c \times \frac{h}{2} \times \frac{w}{2}} \quad \text{and} \quad X^H \in \mathbb{R}^{(1-\alpha)c \times h \times w}. \quad (2)$$

One of the benefits of the new feature representation is the reduction of the spatial redundancy and the compactness compared with the original representation. Furthermore, octave convolution enable efficient communication between the high and the low frequency component of the feature representation.

3.2. Model Architecture

In our work, we have replaced in the architecture all the standard convolutional with the octave convolutional layers as in [5]. Such a change has almost no consequences on the architecture elements since it has been designed in a generic way making it a plug-and-play component. However, octave convolution has some impact on batch normalization layers. This regularization technique expects to have as input the same amount of activations from the feature maps. Because of the octave convolution nature, the size of feature maps will diverge between low and high frequency maps. To cope with this issue, two independent batch normalizations will be deployed, one for the low and one for the high frequency feature maps.

The new hyper-parameter α plays an important role in our architecture since the variation of it involves a change of topology. Motivated by having a similar effect without altering the topology, we define a new set of two hyper-parameters β_L and β_H . These β s allow also to control the influence of low and high frequency feature maps at epoch

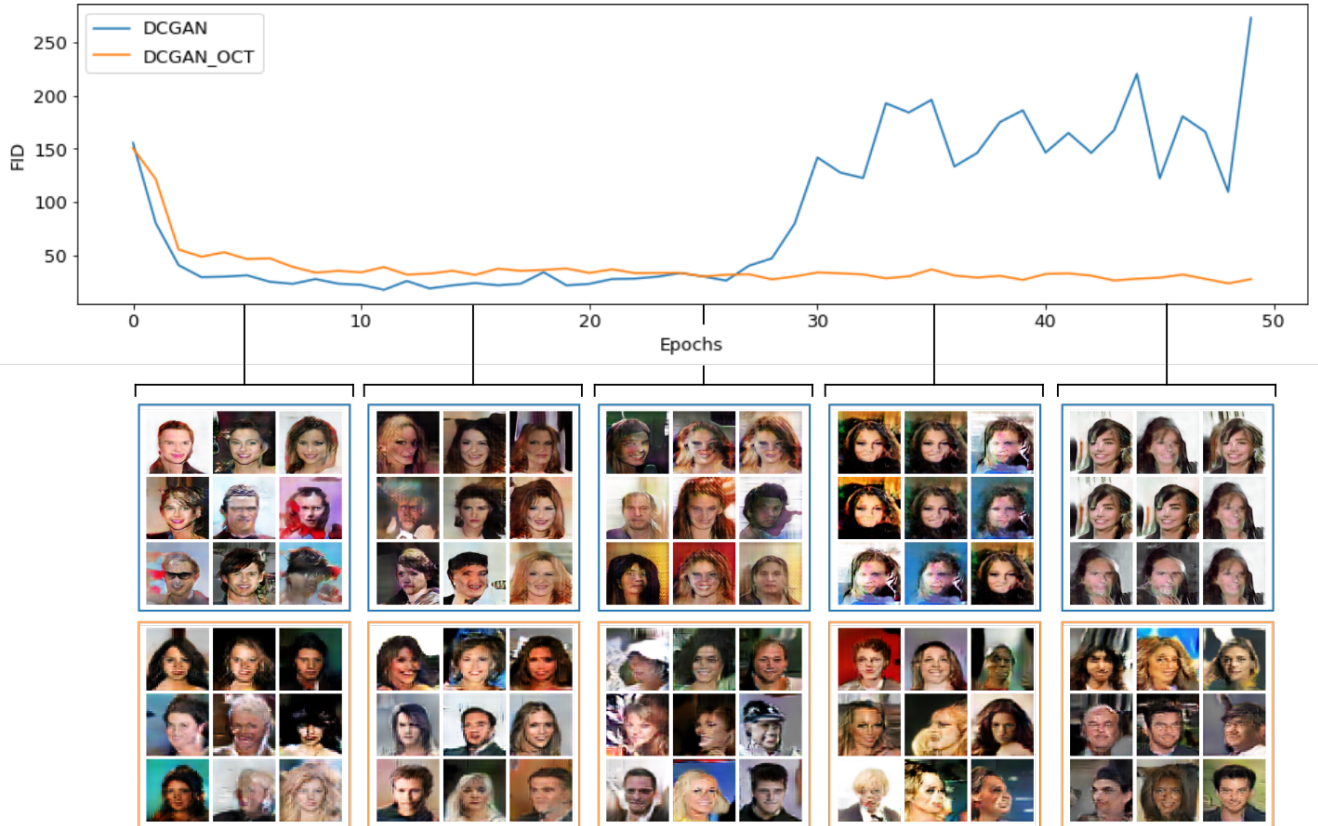


Figure 3: The figure shows the FID evolution together with some random generated examples using a standard DCGAN and its octave variant implementation (DCGAN_OCT).

during training, without modifying the amount of feature maps. Indeed, they can be seen as an extension or substitution of α by a weighting technique on the feature maps (see Figure 7). It can be written in the following manner

$$\beta_L X^L \quad \text{and} \quad \beta_H X^H. \quad (3)$$

4. Experiments

In this section, we present results for a series of experiments evaluating the effectiveness and efficiency of proposed OC-GAN. We first give a detailed introduction of the experimental setup. Then, we discuss the results on several variations of GAN, and finally we explore different configurations modifying the weight of low and high frequency feature maps accordingly. Code is available on Github: <https://github.com/cc-hpc-itwm/Stabilizing-GANs-with-Octave-Convolutions>.

4.1. Experimental Settings

We train OC-GAN on the CelebFaces Attributes (CelebA) dataset [22]. It consists of 202,599 celebrity face

images with variations in facial attributes. In training, we crop and resize the initially 178x218 pixel image to 128x128 pixels. All experiments presented in this paper have been conducted on a single NVIDIA GeForce GTX 1080 GPU, without applying any post-processing. Our evaluation metric is Fréchet Inception Distance (FID) [13], which uses the Inception-v3 network pre-trained on ImageNet to extract features from an intermediate layer. Then, we model the distribution of these features using a multivariate Gaussian distribution with mean μ and covariance Σ . This procedure is conducted for both real images x and generated images z , and it can be written as

$$\text{FID}(x, z) = \|\mu_x - \mu_z\|_2^2 + \text{Tr}(\Sigma_x + \Sigma_z - 2(\Sigma_x \Sigma_z)^{\frac{1}{2}}). \quad (4)$$

Lower FID is better, corresponding to more similar real and generated samples as measured by the distance between their feature distributions.

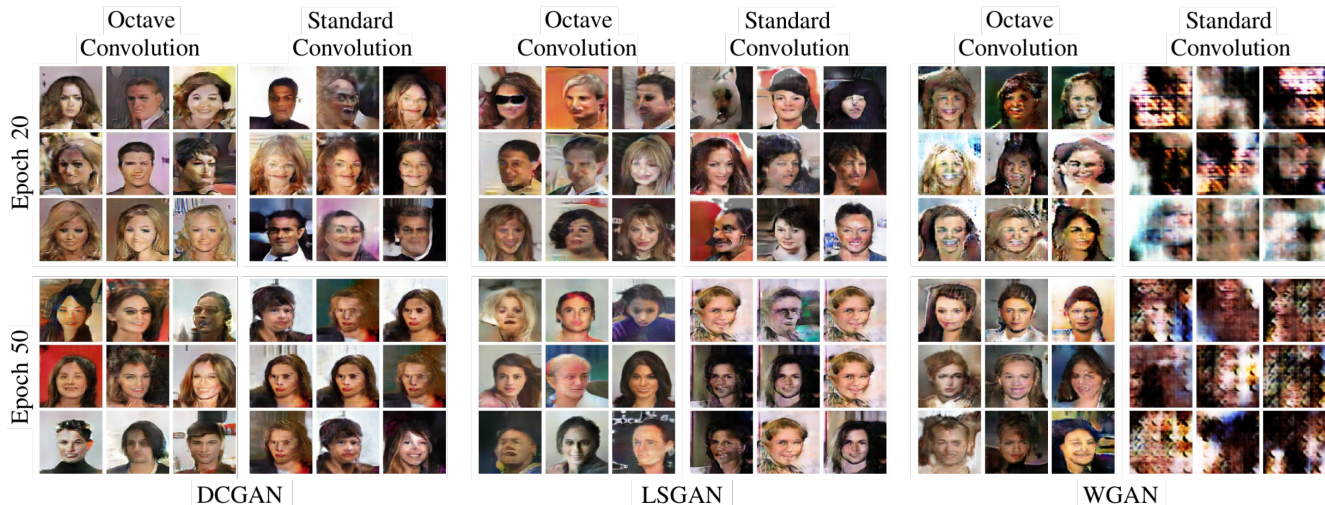


Figure 4: The figure shows three independent blocks belonging to the three different baselines used in the experiments so far. Each block contains several samples across two dimensions components: the horizontal and the vertical. The first refers to the type of convolution implemented, and the second represents the stage of the training (epoch) in the particular baseline.

4.2. Training

In this subsection, we investigate the impact of replacing the standard convolution with octave convolution. We conduct a series of studies using well-known GAN baselines which we have not optimized towards the dataset since the main objective here is to verify the impact of the new convolutional scheme and not to defeat state-of-the-art score results. In particular, we constrain our experiments to three types of GANs: DCGAN, LSGAN and WGAN. All comparisons between the baseline methods and the proposals have the same training and testing setting. We use an Adam optimizer [16] with $\beta_1 = 0.5$, $\beta_2 = 0.999$ during training in all the cases. We set the batch size to 64 and run the experiments for 50 epochs. We update the generator after every discriminator update, and the learning rate used in the implementation is 0.0002.

Standard Octave Convolution. First, we conduct a set of experiments to validate the effect of the octave convolution. Therefore, we set the α to 0.5. We begin with using the baseline models and compute the FID after each iteration. Then, we repeat the same procedure but this time we train using the octave convolution on the models. Our results in Figure 2 show that in all three baselines, the octave model generates images of better or similar quality compared to the previous training. Moreover, we can observe the improvement of stability during training for the octave implementation.

Figure 3 depicts again the comparison between the vanilla DCGAN with the octave version. However, this time the plot includes an arbitrary set of samples which



Figure 5: The figure compares two set of random generated images using DCGAN with octave convolution but different α s. (Top) Implemented with $\alpha = 0.5$. (Bottom) Implemented with $\alpha = 0.99$. The bigger the α is, the less amount of high frequency components are present.

clearly show that these curves correlate well with the visual quality of the generated samples. Even more detailed and extended qualitative evaluations are presented in Figure 4, where numerous samples from all the baselines are displayed. Note that vanilla DCGAN and LSGAN start to suffer from mode collapse from epoch 25 forward. Thus, we choose epoch 20 to do a fair qualitative comparison as

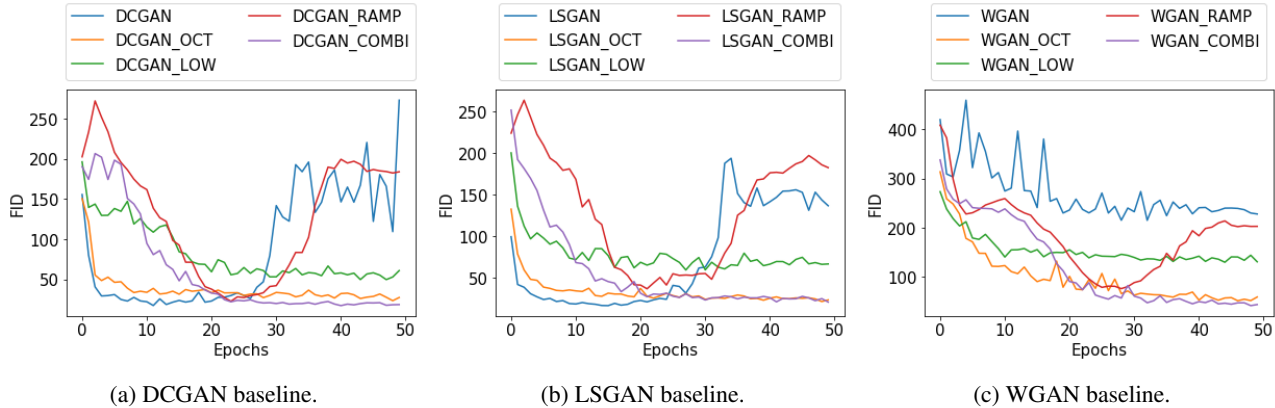


Figure 6: The figures show the FID evolution along the training using different GAN implementation and their octave variants. The suffixes stand for the following: OCT octave convolution with $\alpha = 0.5$ (vanilla configuration), LOW octave convolution with $\alpha = 0.99$, RAMP octave convolution with $\alpha = 0.5$ and β_s as in 7a, and COMBI octave convolution with $\alpha = 0.5$ and β_s as in 7b.

it seems to be the optimal training epoch. We also show the final results (epoch 50), which support the stability claim held in this work.

Feature Maps Weight Search. In this second part of the experiments, we conduct an analysis of the impact of the low and high frequency feature maps. In order to verify how sensitive GANs are to these modifications, we start running a test for the three baselines, where we set α to 0.99¹ (see Figure 5). By doing so, we get rid of all the high frequency maps, and as it is expected, the training shows constant stability since low frequencies do not contain big jumps or variations. On the other hand, surprisingly the score results are not dramatically worse than vanilla baselines (see Figure 6). Indeed, it is interesting to notice that both share a similar FID score evolution.

From the previous results, we notice the importance of hyper-parameter α . However, it is a well-known NP-hard problem to find the best topology in deep neural networks and in fact, it is an area of active research by itself [8, 21, 34]. As a consequence, we avoid to modify directly the topology by changing α . Driven by these observations, finally, we conduct a new series of experiments based on two new hyper-parameters β_L and β_H . Indeed, they can be seen as an extension of α because they will modify the feature maps too. Nonetheless, β_s do not modify the amount of feature maps, but their weight. In Figure 7 are plotted two different strategies followed in the work. On the one hand, we implement a ramp scheme (see Figure 7a). The intuition behind is that low frequency signals that capture the global layout and coarse structure are learnt at the

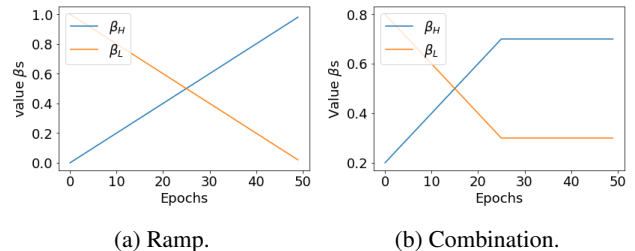


Figure 7: The figures show the weight β_s evolution along the epochs using a ramp (a) and a combination (b) scheme.

beginning, and after a certain time the high frequency parts that capture fine details, start to appear and gain more importance. Trying to capture such a behaviour, we deploy the ramp evolution. Nonetheless, this strategy might be too harsh as the role played by the low and high frequencies is too insignificant at certain training stages (see Figure 6). As a result, on the other hand, we implement a second weighting strategy called combination (see Figure 7b), which tries to be a trade-off between frequency components offering an optimized combination. In Figure 6 are shown the three baselines and their octave variants.

5. Conclusions

In this work, we tackle the problem of stability during GANs training. We propose a novel and simple framework coined as OC-GAN because of its octave convolution implementation. We show how this method is orthogonal and complementary to existing methods and leads to generate images of better or equal quality suppressing the mode collapse problem. We see many interesting avenues of future work including exploring Bayesian optimizations.

¹We cannot set α to 1 because of implementation issues. Nevertheless, the difference should be negligible.

References

- [1] Martin Arjovsky, Soumith Chintala, and Léon Bottou. Wasserstein gan. *arXiv preprint arXiv:1701.07875*, 2017.
- [2] Andrew Brock, Jeff Donahue, and Karen Simonyan. Large scale gan training for high fidelity natural image synthesis. *arXiv preprint arXiv:1809.11096*, 2018.
- [3] Fergus W Campbell and JG Robson. Application of fourier analysis to the visibility of gratings. *The Journal of physiology*, 197(3):551–566, 1968.
- [4] Liang-Chieh Chen, George Papandreou, Iasonas Kokkinos, Kevin Murphy, and Alan L Yuille. Deeplab: Semantic image segmentation with deep convolutional nets, atrous convolution, and fully connected crfs. *IEEE transactions on pattern analysis and machine intelligence*, 40(4):834–848, 2017.
- [5] Yunpeng Chen, Haoqi Fang, Bing Xu, Zhicheng Yan, Yannis Kalantidis, Marcus Rohrbach, Shuicheng Yan, and Jiashi Feng. Drop an octave: Reducing spatial redundancy in convolutional neural networks with octave convolution. *arXiv preprint arXiv:1904.05049*, 2019.
- [6] François Chollet. Xception: Deep learning with depthwise separable convolutions. In *Proceedings of the IEEE conference on computer vision and pattern recognition*, pages 1251–1258, 2017.
- [7] Russell L DeValois and Karen K DeValois. *Spatial vision*. Oxford university press, 1990.
- [8] Thomas Elsken, Jan Hendrik Metzen, and Frank Hutter. Neural architecture search: A survey. *arXiv preprint arXiv:1808.05377*, 2018.
- [9] Ross Girshick, Jeff Donahue, Trevor Darrell, and Jitendra Malik. Rich feature hierarchies for accurate object detection and semantic segmentation. In *Proceedings of the IEEE conference on computer vision and pattern recognition*, pages 580–587, 2014.
- [10] Ian Goodfellow, Jean Pouget-Abadie, Mehdi Mirza, Bing Xu, David Warde-Farley, Sherjil Ozair, Aaron Courville, and Yoshua Bengio. Generative adversarial nets. In *Advances in neural information processing systems*, pages 2672–2680, 2014.
- [11] Ishaan Gulrajani, Faruk Ahmed, Martin Arjovsky, Vincent Dumoulin, and Aaron C Courville. Improved training of wasserstein gans. In *Advances in Neural Information Processing Systems*, pages 5767–5777, 2017.
- [12] Song Han, Jeff Pool, Sharan Narang, Huizi Mao, Enhao Gong, Shijian Tang, Erich Elsen, Peter Vajda, Manohar Paluri, John Tran, et al. Dsd: Dense-sparse-dense training for deep neural networks. *arXiv preprint arXiv:1607.04381*, 2016.
- [13] Martin Heusel, Hubert Ramsauer, Thomas Unterthiner, Bernhard Nessler, and Sepp Hochreiter. Gans trained by a two time-scale update rule converge to a local nash equilibrium. In *Advances in Neural Information Processing Systems*, pages 6626–6637, 2017.
- [14] Tero Karras, Timo Aila, Samuli Laine, and Jaakko Lehtinen. Progressive growing of gans for improved quality, stability, and variation. *arXiv preprint arXiv:1710.10196*, 2017.
- [15] Tsung-Wei Ke, Michael Maire, and Stella X Yu. Multigrid neural architectures. In *Proceedings of the IEEE Conference on Computer Vision and Pattern Recognition*, pages 6665–6673, 2017.
- [16] Diederik P Kingma and Jimmy Ba. Adam: A method for stochastic optimization. *arXiv preprint arXiv:1412.6980*, 2014.
- [17] Diederik P Kingma and Max Welling. Auto-encoding variational bayes. *arXiv preprint arXiv:1312.6114*, 2013.
- [18] Alex Krizhevsky, Ilya Sutskever, and Geoffrey E Hinton. Imagenet classification with deep convolutional neural networks. In *Advances in neural information processing systems*, pages 1097–1105, 2012.
- [19] Yann LeCun, Léon Bottou, Yoshua Bengio, Patrick Haffner, et al. Gradient-based learning applied to document recognition. *Proceedings of the IEEE*, 86(11):2278–2324, 1998.
- [20] Chieh Hubert Lin, Chia-Che Chang, Yu-Sheng Chen, Da-Cheng Juan, Wei Wei, and Hwann-Tzong Chen. Cogan: Generation by parts via conditional coordinating. *arXiv preprint arXiv:1904.00284*, 2019.
- [21] Hanxiao Liu, Karen Simonyan, and Yiming Yang. Darts: Differentiable architecture search. *arXiv preprint arXiv:1806.09055*, 2018.
- [22] Ziwei Liu, Ping Luo, Xiaogang Wang, and Xiaoou Tang. Deep learning face attributes in the wild. In *Proceedings of the IEEE international conference on computer vision*, pages 3730–3738, 2015.
- [23] Jonathan Long, Evan Shelhamer, and Trevor Darrell. Fully convolutional networks for semantic segmentation. In *Proceedings of the IEEE conference on computer vision and pattern recognition*, pages 3431–3440, 2015.
- [24] Jian-Hao Luo, Jianxin Wu, and Weiyao Lin. Thinet: A filter level pruning method for deep neural network compression. In *Proceedings of the IEEE international conference on computer vision*, pages 5058–5066, 2017.
- [25] Xudong Mao, Qing Li, Haoran Xie, Raymond YK Lau, Zhen Wang, and Stephen Paul Smolley. Least squares generative adversarial networks. In *Proceedings of the IEEE International Conference on Computer Vision*, pages 2794–2802, 2017.
- [26] Takeru Miyato, Toshiki Kataoka, Masanori Koyama, and Yuichi Yoshida. Spectral normalization for generative adversarial networks. *arXiv preprint arXiv:1802.05957*, 2018.
- [27] Aaron van den Oord, Nal Kalchbrenner, and Koray Kavukcuoglu. Pixel recurrent neural networks. *arXiv preprint arXiv:1601.06759*, 2016.
- [28] Alec Radford, Luke Metz, and Soumith Chintala. Unsupervised representation learning with deep convolutional generative adversarial networks. *arXiv preprint arXiv:1511.06434*, 2015.
- [29] Joseph Redmon, Santosh Divvala, Ross Girshick, and Ali Farhadi. You only look once: Unified, real-time object detection. In *Proceedings of the IEEE conference on computer vision and pattern recognition*, pages 779–788, 2016.
- [30] Shaoqing Ren, Kaiming He, Ross Girshick, and Jian Sun. Faster r-cnn: Towards real-time object detection with region proposal networks. In *Advances in neural information processing systems*, pages 91–99, 2015.

- [31] Olaf Ronneberger, Philipp Fischer, and Thomas Brox. U-net: Convolutional networks for biomedical image segmentation. In *International Conference on Medical image computing and computer-assisted intervention*, pages 234–241. Springer, 2015.
- [32] Karen Simonyan and Andrew Zisserman. Very deep convolutional networks for large-scale image recognition. *arXiv preprint arXiv:1409.1556*, 2014.
- [33] Saining Xie, Ross Girshick, Piotr Dollár, Zhuowen Tu, and Kaiming He. Aggregated residual transformations for deep neural networks. In *Proceedings of the IEEE conference on computer vision and pattern recognition*, pages 1492–1500, 2017.
- [34] Saining Xie, Alexander Kirillov, Ross Girshick, and Kaiming He. Exploring randomly wired neural networks for image recognition. *arXiv preprint arXiv:1904.01569*, 2019.